0026-895X/11/8003-466–475$25.00
MOLECULAR PHARMACOLOGY
Vol. 80, No. 3
70862/3705821
Mol Pharmacol 80:466–475, 2011
Printed in U.S.A.

Off-Target Serine/Threonine Kinase 10 Inhibition by Erlotinib Enhances Lymphocytic Activity Leading to Severe Skin Disorders

Naoko Yamamoto, Masashi Honma, and Hiroshi Suzuki

Department of Pharmacy, the University of Tokyo Hospital, Faculty of Medicine, the University of Tokyo, Tokyo Japan

Received December 23, 2010; accepted May 23, 2011

ABSTRACT

Skin disorders are among the most common adverse events related to treatment with epidermal growth factor receptor (EGFR) kinase inhibitors, and of these, erlotinib is known to cause more frequent and severe skin disease than other agents in this class. Although previous reports have shown that cutaneous manifestations are triggered by the inhibition of multiple EGFR-related homeostatic functions of the skin, this mechanism alone cannot explain the differences in frequency and severity of skin disorders caused by different kinase inhibitors. In this study, we focused on the relationship between the off-target kinase inhibition and aggravation of skin disorders. Based on calculations using reported K_d values and plasma drug concentrations, serine/threonine kinase 10 (STK10) and Ste20-like kinase (SLK) were selected as candidates preferentially inhibited by erlotinib over gefitinib. In vitro experiments confirmed that STK10 and SLK kinase activity are inhibited by erlotinib at clinical concentrations, whereas only STK10 is slightly inhibited by gefitinib. It was also shown that erlotinib up-regulated lymphocytic responses such as interleukin (IL)-2 secretion and cell migration at clinical concentrations, whereas gefitinib did not affect lymphocyte activity. Moreover, small interfering RNA experiments revealed that STK10 plays a major role in up-regulation of the lymphocytic responses induced by erlotinib treatment. Finally, the role of erlotinib-induced lymphocyte activation was assessed in vivo using irritant hypersensitivity models. The results indicated that erlotinib aggravates cutaneous inflammatory reactions through the activation of lymphocytic responses such as IL-2 secretion and cell migration. These results demonstrated that off-target inhibition of STK10 by erlotinib enhances lymphocytic responses, which lead to the aggravation of skin inflammation.

Introduction

Erlotinib and gefitinib are low-molecular-weight tyrosine kinase inhibitors. Their primary target is epidermal growth factor receptor (EGFR), and they have been used to treat patients with non–small-cell lung cancer (Kris et al., 2003; Shepherd et al., 2005). In addition to erlotinib and gefitinib, other kinase inhibitors and monoclonal antibodies that target EGFR, including lapatinib, cetuximab, and panitumumab, have also been developed and used for the treatment of various types of cancer (Bonner et al., 2006; Geyer et al., 2006; Van Cutsem et al., 2007). Skin disorders, including rash, pruritus, dry skin, and acne, are among the most common adverse events observed in patients treated with these drugs (Albanell et al., 2002; Segaert and Van Cutsem, 2005). After a week of treatment with erlotinib or gefitinib, acneiform eruptions with severe pain and itching appear primarily on the face and upper trunk (Hidalgo et al., 2001; Pallis et al., 2003). These symptoms can worsen a patient's quality of life and can lead to the dose reduction or discontinuation of treatment with EGFR inhibitory agents (Shepherd et al., 2005).

Many studies have examined the relationship between EGFR inhibition and the development of cutaneous side effects (Albanell et al., 2002; Guttman-Yassky et al., 2010). Inhibition of EGFR-mediated signaling pathways induces multiple effects in basal keratinocytes, including growth arrest, decreased migration, increased cell attachment, abnor-

This work was supported in part by Grant-in-Aid for Scientific Research [Grant 21390041] and Grant-in-Aid for Scientific Research on Innovative Areas HD-Physiology [Grant 22136015] from the Ministry of Education, Science, and Culture of Japan.

Article, publication date, and citation information can be found at http://molpharm.aspetjournals.org.

doi:10.1124/mol.110.070862.

ABBREVIATIONS: EGFR, epidermal growth factor receptor; FBS, fetal bovine serum; GAK, cyclin G-associated kinase; MEK1, mitogen-activated protein kinase extracellular signal-regulated kinase kinase-1; PMA, phorbol 12-myristate 13-acetate; SDF-1, stromal cell-derived factor-1; SLK, Ste20-like kinase; STK10, serine/threonine kinase 10; IL, interleukin; PCR, polymerase chain reaction; LC, liquid chromatography; MS/MS, tandem mass spectrometry; ERK, extracellular signal-regulated kinase; TCR, T-cell receptor; siRNA, small interfering RNA; FTY720, 2-amino-2-[2-(4-octylphenyl)ethyl]-1,3-propanediol, hydrochloride; RNAi, RNA interference; PD98059, 2′-amino-3′-methoxyflavone.

mal differentiation, apoptosis, and stimulation of inflammatory systems, all of which result in distinctive cutaneous manifestations (Kari et al., 2003; Mascia et al., 2003; Woodworth et al., 2005). However, the prevalence and severity of drug-related skin disorders vary significantly among EGFR kinase inhibitors. In Japanese patients, the frequency of rash was higher in patients receiving erlotinib (97%) (Tarceva, Japanese package insert, 2010; Chugai Pharmaceutical Corp, Tokyo, Japan) than in those on gefitinib (63%) (Iressa, Japanese package insert, 2010; AstraZeneca, Osaka, Japan). Lapatinib, a dual EGFR and human epidermal growth factor receptor 2 tyrosine kinase inhibitor used for the treatment of human epidermal growth factor receptor 2-positive breast cancer, was reported to induce rash in 49.8% of patients receiving monotherapy (Toi et al., 2009). In addition, rash severity also differs in patients taking erlotinib versus gefitinib. In phase I/II studies of erlotinib in the Japanese population, the frequency of rash graded using the National Cancer Institute Common Terminology Criteria for Adverse Events levels G2 and G3 was 67 and 4%, respectively (Tarceva Japanese package insert), whereas in phase II trial of gefitinib in patients composed of Japanese and non-Japanese patients, the frequency of rash graded G2 and G3 was 19 and 1%, respectively (Fukuoka et al., 2003). Moreover, the IC_{50} values for erlotinib, gefitinib, and lapatinib were reported to be 2, 23, and 11 nM, respectively (Moyer et al., 1997; Rusnak et al., 2001; Albanell et al., 2002). Considering the steady-state unbound plasma concentrations of each drug under clinical conditions, it is estimated that EGFR is almost completely inhibited in each case. This suggests that factors other than EGFR inhibition also contribute to the severe cutaneous side effects of erlotinib.

A few reports have described the unanticipated effects caused by the inhibition of off-target kinases. Although imatinib was designed to specifically target BCR-Abl, a gene product that causes chronic myeloid leukemia, it has been suggested that imatinib has direct effects on bone-resorbing osteoclasts and bone-forming osteoblasts through the off-target inhibition of c-fms, c-kit, carbonic anhydrase II, and platelet-derived growth factor receptor (Vandyke et al., 2010). In another example, sunitinib, a multitarget kinase inhibitor used to treat renal cell carcinoma and gastrointestinal stromal tumor, inhibits a number of growth factor receptors regulating both tumor cell proliferation and tumor angiogenesis (Guttman-Yassky et al., 2010). It has been suggested that the off-target inhibition of 5′-AMP-activated protein kinase plays a central role in sunitinib toxicity in cardiomyocytes (Kerkela et al., 2009).

Karaman et al. (2008) have reported comprehensive measurement of selectivity of kinase inhibitors. That analysis revealed that both gefitinib and erlotinib interact with several off-target kinases and with their primary target, EGFR. However, it is still unclear whether off-target inhibition by erlotinib or gefitinib plays a role in cutaneous side effects of these drugs. Here, to test that possibility, we compared off-target inhibition profiles of gefitinib and erlotinib at the steady-state unbound plasma concentrations found under clinical conditions. Our findings suggest that the off-target serine/threonine kinase 10 (STK10) is inhibited much more potently by erlotinib than by gefitinib under clinical conditions. Furthermore, in vitro experiments showed that erlotinib enhances lymphocytic responses such as cell migration and interleukin-2 (IL-2) secretion via STK10 inhibition. Our in vivo observations were consistent with these in vitro results. These results suggest that erlotinib exacerbates skin disorders through off-target kinase inhibition.

Materials and Methods

Cell Lines. 293FT cells were obtained from Invitrogen (Carlsbad, CA) and cultured in Dulbecco's modified Eagle's medium (Nacalai Tesque, Kyoto, Japan) supplemented with 10% fetal bovine serum, 2 mM L-glutamine, and 100 μg/ml penicillin and streptomycin (Invitrogen). Jurkat E6-1 cells were obtained from the American Type Culture Collection (Manassas, VA) and cultured in RPMI 1640 medium (Nacalai Tesque) supplemented with 10% fetal bovine serum and 100 μg/ml penicillin and streptomycin.

Animals. Male ddY mice were purchased from Japan SLC Inc. (Hamamatsu, Japan). Mice were allowed to acclimate to housing conditions for at least 7 days before handling and were analyzed at 6 weeks of age. All animal procedures were approved by the Institutional Animal Care and Use Committee of Graduate School of Medicine, the University of Tokyo.

Calculation of Occupancy Rates. Mean occupancy rate (R) of the kinase by the drug under clinical conditions was calculated according to the Michaelis-Menten-type equation $R = C_{p,u,ss}/(K_d + C_{p,u,ss})$, where $C_{p,u,ss}$ and K_d are the steady-state mean unbound plasma concentration of the drug obtained from Japanese package insert and the dissociation constant of the drug from the kinase obtained from a previous report (Karaman et al., 2008), respectively.

Preparation of Recombinant Kinase. Genes encoding human STK10 and Ste20-like kinase (SLK) were cloned using cDNA from MCF-7 cells and Jurkat E6-1 cells, respectively. Genes encoding mouse STK10 and SLK were cloned using cDNA from mouse spleens and mouse brains, respectively. Each gene was fused with a histidine tag at the N terminus and subcloned into the pcDNA3.3 vector (Invitrogen) to produce 6-His STK10/pcDNA3.3 and 6-His SLK/pcDNA3.3. 293FT cells were transfected with 6-His STK10/pcDNA3.3 or 6-His SLK/pcDNA3.3 using Lipofectamine 2000 (Invitrogen) according to the manufacturer's protocol. Forty-eight hours after transfection, cells were lysed in a lysis buffer (phosphate-buffered saline, pH 8.0) containing 1% Nonidet P-40 (Nacalai Tesque, Kyoto, Japan) and a protease inhibitor cocktail (Roche Diagnostics, Indianapolis, IN). The recombinant proteins were purified using Profinity IMAC Ni-Charged Resin (Bio-Rad Laboratories, Tokyo, Japan).

In Vitro Kinase Assay. To measure the kinase activity of STK10 and SLK, 100 ng of each recombinant protein was incubated with 1 μg of myelin basic protein (Millipore Biosciences Research Reagents, Temecula, CA) and 1 μM ATP in kinase buffer (20 mM HEPES, 10 mM $MgCl_2$, 3 mM $MnCl_2$, and 0.1 mg/ml bovine serum albumin, pH 7.6) for 1 h at 37°C. The remaining ATP concentration was determined using the Kinase-Glo Plus Luminescent Kinase Assay (Promega, Madison, WI) according to the manufacturer's protocol. To determine the IC_{50} values for gefitinib and erlotinib for each kinase, each compound was added to the reaction mixture at the indicated concentrations. ATP concentrations were fitted to the standard IC_{50} model, and IC_{50} values were determined based on Powell's nonlinear least square method with a uniform weighting factor using Scientist software (MicroMath, Salt Lake City, UT).

Small Interfering RNA. siRNA was designed against human STK10 and SLK using BLOCK-iT RNAi Designer (Invitrogen). Sequences were 5′-GCC UGU CUA CCU UCG AGA A-3′ for STK10 (siSTK10) and 5′-GCC AUA ACC AGA ACC UGA A-3′ for SLK (siSLK). siRNA duplexes containing a di-deoxythymine overhang at the 3′ terminus were synthesized (Sigma-Aldrich, St. Louis, MO). Each siRNA duplex was introduced into Jurkat E6-1 cells by electroporation using a Gene Pulser Xcell (Bio-Rad Laboratories) at a setting of 140 V, 1000 μF, and using a 0.1-cm gap cuvette according

to the manufacturer's protocol. As a negative control (siNeg), we used siPerfect Negative Control (Sigma-Aldrich) that contains at least three miss-matches against human, mouse, and rat genes.

Quantification of mRNA Expression by Real-Time PCR. Total RNA was extracted from Jurkat E6-1 cells using RNAsolv (Omega Bio-Tek, Lilburn, GA) according to the manufacturer's protocol, and the prepared RNA was reverse-transcribed with ReverTra Ace (Toyobo Engineering, Osaka, Japan). Quantitative real-time PCR was performed using SYBR GreenER qPCR SuperMix Universal (Invitrogen), a Chromo4 (Bio-Rad Laboratories), and the associated software. Primers used for the quantification of gene expression were as follows: human STK10: forward, 5′-ATC CTG CGC CTG TCT ACC TT-3′; reverse, 5′-GCC TTG TAA ACC TTG CCG AA-3′; human SLK: forward, 5′-CCT CAG CCT GTT CTA ATA CCC A-3′; reverse, 5′-GGA TTC TCA GAT TCT GGT GGC A-3′; human IL-2: forward, 5′-TCC TGT CTT GCA TTG CAC TAA G-3′; reverse, 5′-CAT CCT GGT GAG TTT GGG ATT C-3′; and β-actin: forward, 5′-CCG GAA GGA AAA CTG ACA GC-3′; reverse, 5′-GTG GTG GTG AAG CTG TAG CC-3′. The relative expression level of each gene was normalized to that of β-actin.

Western Blotting. Forty-eight hours after siRNA introduction into Jurkat E6-1 cells, whole cell lysates were prepared with phosphate-buffered saline containing 1% NP-40 (lysis buffer). Proteins (20 μg/lane) were separated on 7.5% of SDS-polyacrylamide gels and transferred onto Immobilon membranes (Millipore Corporation, Billerica, MA). After a blocking treatment with Tris-buffered saline containing 3% bovine serum albumin, membranes were incubated with anti-human STK10 antibody or anti-human SLK antibody (BETHYL, Montgomery, TX) as primary antibodies. As the secondary antibody, anti-rabbit IgG antibody labeled with horseradish peroxidase (GE Healthcare, Chalfont St. Giles, Buckinghamshire, UK) was used. ECL Plus (GE Healthcare) was used for detection according to the manufacturer's protocol and analyzed using a Chemidoc XRS (Bio-Rad Laboratories).

Measurement of IL-2 by Enzyme-Linked Immunosorbent Assay. Jurkat E6-1 cells were seeded on a 96-well plate at a density of 10^5 cells/well for stimulation with Dynabeads Human T-Activator CD3/CD28 (Veritas, Tokyo, Japan) at a ratio of three beads to one cell. Lymph node cells isolated from ddY mice were seeded on a 96-well plate at a density of 10^5 cells/well for stimulation with Dynabeads Mouse T-Activator CD3/CD28 (Veritas) at a ratio of one bead to one cell. For costimulation experiments with PMA (20 ng/ml) and ionomycin (1 μM), both Jurkat cells and lymph node cells were seeded at a density of 2×10^5 cells/well. The indicated concentrations of gefitinib, erlotinib, and/or 2′-amino-3′-methoxyflavone (PD98059; 50 μM) were added to the media at 1 h before beads stimulation. In the siRNA experiments, we added erlotinib or gefitinib to the media at unbound concentrations of 400 and 150 nM, respectively, which are around the maximum unbound plasma concentrations of these drugs. Cell culture supernatants were collected 48 h after stimulation, and IL-2 concentration was measured by using the Quantikine Human IL-2 immunoassay (R&D Systems, Minneapolis, MN) according to the manufacturer's protocol.

Measurement of IL-2 mRNA. Jurkat E6-1 cells were seeded on a 12-well plate at a density of 4×10^5 cells/well. Bead stimulation and treatment with gefitinib and erlotinib were performed as described above. Cell pellets were collected 5 h after bead stimulation, and IL-2 mRNA was measured using quantitative PCR.

Cell Migration Assay. Jurkat E6-1 cells were serum-starved, and gefitinib or erlotinib were added to the medium at the indicated concentrations 1 h before the cell migration assay. The migration assay was performed using a transwell system with a polycarbonate membrane with a 5-μm pore (Corning Life Sciences, Lowell, MA). Jurkat E6-1 cells were seeded on the upper chamber of each transwell at a density of 10^7 cells/well, and the lower chamber was filled with medium containing 10 ng/ml stromal cell-derived factor-1 (SDF-1; PeproTech, Rocky Hill, NJ) and 0.1 mg/ml bovine serum albumin. Gefitinib and erlotinib were added to the top and bottom chambers at the indicated concentrations. Cells were incubated at 37°C for 2 h, and cells that migrated into the lower chamber were counted with a hemocytometer. For gene knockdown experiments, the cell migration assay was performed 24 h after the addition of siRNA. SDF-1 was added at a concentration of 30 ng/ml.

Quantification of Erlotinib and Gefitinib Using LC-MS/MS. LC-MS/MS analyses were conducted using a Quattro Premier XE Tandem Quadrupole Mass Spectrometer coupled to an ACQUITY Ultra Performance LC System with an integral autoinjector (Waters, Milford, MA). The Premier XE was run in the electrospray ionization-positive MS/MS multiple reaction-monitoring mode at a source temperature of 120°C and a desolvation temperature of 350°C by monitoring the following mass transitions (parent-to-daughter ion): *m/z* 447.43 to 127.8 for gefitinib, *m/z* 394.43 to 278.2 for erlotinib, and *m/z* 268.23 to 116.03 for metoprolol, which was used as an internal standard. The cone voltage was set at 45 V for gefitinib, 55 V for erlotinib, and 35 V for metoprolol. Plasma samples were deproteinized with four volumes of acetonitrile (Nacalai Tesque), and the supernatants were separated on an ACQUITY UPLC BEH Shield RP18 1.7-μm, 2.1 × 100-mm column (Waters) with a flow rate of 0.4 ml/min and a binary solvent system of water-acetonitrile containing 0.1% formic acid. Data analyses were carried out using MassLynx software (version 4.1) and quantified using sample peak area.

Pharmacokinetic Analysis. Each mouse was orally administered erlotinib (t = 0 h, 18 mg/kg; t = 6, 12, and 18 h, 13 mg/kg) or gefitinib (t = 0 h, 25 mg/kg; t = 6, 12, and 18 h, 18 mg/kg) dissolved in saline containing 25% methyl-β-cyclodextrin (Wako Pure Chemicals, Osaka, Japan). This dosing schedule was designed to sustain the inhibition rate of mouse STK10 by erlotinib or gefitinib in ddY mice at a level comparable with that of human STK10 under clinical conditions. The STK10 inhibition rate at each time point was calculated based on the IC_{50} values determined from in vitro kinase assays and the plasma concentration of erlotinib or gefitinib, which was measured using LC-MS/MS. Plasma samples were collected from the jugular vein at the indicated times. Plasma proteins were precipitated with four volumes of acetonitrile, and the supernatants were evaporated at 40°C under nitrogen gas flow. The pellets were dissolved in 10% acetonitrile and used for quantification.

Irritant Dermatitis Model. Each mouse was orally administered erlotinib (t = 0 h, 18 mg/kg; t = 6, 12, and 18 h, 13 mg/kg) or gefitinib (t = 0 h, 25 mg/kg; t = 6, 12, and 18 h, 18 mg/kg) dissolved in saline containing 25% methyl-β-cyclodextrin (Wako Pure Chemicals). To elicit irritant dermatitis, 25 μl of 5% croton oil dissolved in acetone/olive oil [5:1 (v/v)] was applied to both sides of each ear 1 h after the first administration of gefitinib and erlotinib. To evaluate the contribution of IL-2 to dermatitis, 500 μg/kg anti-IL-2 monoclonal antibody (clone JES6-1A12; R&D systems) was injected intravenously just before croton oil treatment. To evaluate the effect of lymphocyte suppression, 3 mg/kg 2-amino-2-[2-(4-octylphenyl)ethyl]-1,3-propanediol, hydrochloride (FTY720; Cayman Chemical, Ann Arbor, MI) was orally administered on days −2, −1, and 0. The degree of earflap swelling was measured 24 h after irritant application. Infiltration of lymphocytes to the earflaps was also quantitated. For this experiment, treatment with erlotinib or gefitinib and irritant application were performed as described above, and mice were sacrificed 6 h after irritant challenge. The earflaps were excised and fixed in phosphate-buffered saline containing 4% paraformaldehyde. The tissues were embedded in paraffin, and then longitudinal thin sections were prepared for staining with hematoxylin-eosin as described previously. In one-third, one-half, and two-thirds distances from the base to the tip of earflap sections along with long axis, areas with 200 μm width were selected, and infiltrated lymphocytes were counted.

Statistical Analyses. All data are expressed as means ± S.D. from at least three independent experiments. Statistical analysis was performed using a Student's t test or an analysis of variance followed by Bonferroni's test where applicable.

Results

Comparison of Off-Target Kinase Occupancy Rates in Erlotinib and Gefitinib at Clinical Levels. To compare the off-target interaction profiles of erlotinib and gefitinib, we calculated their occupancy rates for 317 types of human kinases based on a previous report of high-throughput measurements of the K_d values of various kinase inhibitors for human kinases (Karaman et al., 2008), taking into account the steady-state mean unbound plasma concentration of these agents under clinical conditions (Nakagawa et al., 2003; Yamamoto et al., 2008) (Fig. 1). It was estimated that both erlotinib and gefitinib occupy EGFR almost completely (100% by erlotinib and 99% by gefitinib). Cyclin G-associated kinase (GAK) was also estimated to be highly occupied by both agents (99% by erlotinib and 84% by gefitinib). In contrast, the estimated occupancy rates for STK10 and SLK were much higher for erlotinib than for gefitinib (92% by erlotinib and 12% by gefitinib for STK10, and 89% by erlotinib and 7% by gefitinib for SLK). It has been reported that both STK10 and SLK are members of the Ste20 family of serine/threonine protein kinases, and STK10 is reported to be expressed predominantly in lymphocytes (Walter et al., 2003) and to negatively regulate lymphocytic responses such as IL-2 expression and cell migration (Tao et al., 2002; Belkina et al., 2009). Given that the up-regulation of lymphocytic activity is likely to lead to the aggravation of inflammatory reactions, including skin disorders, we focused on STK10 and SLK in subsequent experiments.

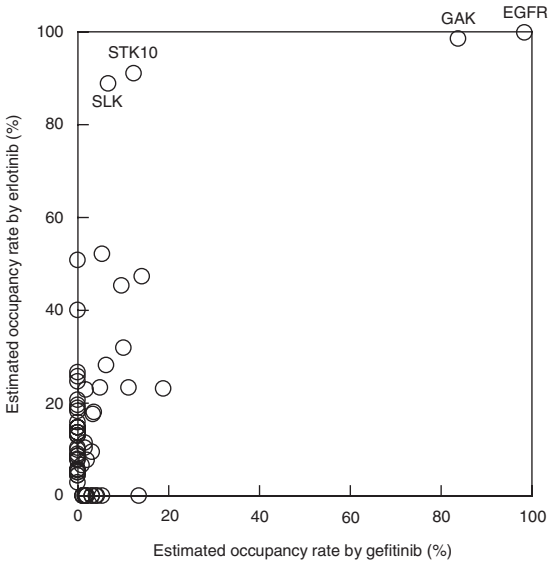

Fig. 1. Comparison of off-target kinase occupancy rates for erlotinib and gefitinib. Occupancy rates were calculated based on the reported K_d values of erlotinib and gefitinib for human kinases and the steady-state mean unbound plasma concentration of these agents under clinical conditions.

Determination of IC_{50} Values for STK10 and SLK by Erlotinib and Gefitinib. To confirm that STK10 and SLK kinase activity was actually inhibited by erlotinib under clinical conditions, we determined the IC_{50} values of erlotinib and gefitinib for human STK10, SLK, and their mouse orthologs using an in vitro kinase assay system (Fig. 2). The results indicated that erlotinib inhibited STK10 and SLK more potently than gefitinib under clinical conditions. The IC_{50} values of erlotinib and gefitinib for human STK10 were 160 and 1300 nM, respectively, and those for mouse STK10 were 350 and 1900 nM, respectively (Fig. 2, A and B). The IC_{50} values of erlotinib and gefitinib for human SLK were 830 and 5200 nM, respectively, and those for mouse SLK were 480 and 1600 nM, respectively (Fig. 2, C and D). Based on these results, it was estimated that the inhibition rate for STK10 is approximately 60% for patients treated with erlotinib, but only 4% for patients treated with gefitinib. The inhibitory effects on SLK were estimated to be somewhat lower than those on STK10, and it was estimated that the inhibition rate was approximately 25% for patients treated with erlotinib and minimal for those treated with gefitinib.

Erlotinib Up-Regulates IL-2 Secretion and Cell Migration Activity in Lymphocytes. As mentioned above, it has been suggested that STK10 negatively regulates lymphocytic activity (Tao et al., 2002; Belkina et al., 2009). Therefore, we speculated that the possibility that the preferential inhibition of STK10 or SLK, which is closely related to

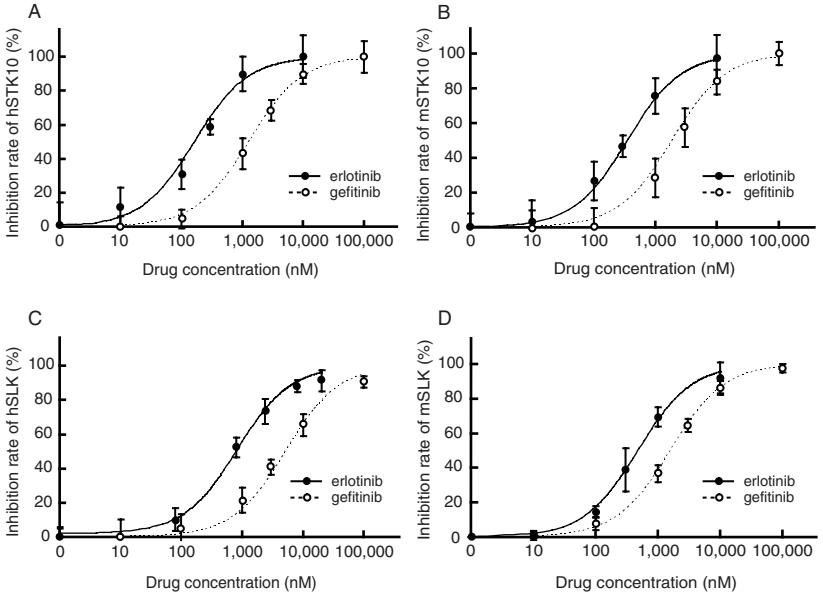

Fig. 2. Determination of IC_{50} values for erlotinib and gefitinib for STK10 or SLK. In vitro kinase assays for hSTK10 (A), mSTK10 (B), hSLK (C), and mSLK (D). Each data point represents the mean ± S.D. (n = 6). IC_{50} values for erlotinib were 160 nM for hSTK10, 830 nM for hSLK, 350 nM for mSTK10, and 480 nM for mSLK. IC_{50} values for gefitinib were 1300 nM for hSTK10, 5200 nM for hSLK, 1900 nM for mSTK10, and 1600 nM for mSLK.

STK10, by erlotinib might enhance lymphocyte action. To compare the effects of erlotinib and gefitinib on lymphocytic IL-2 secretion, we measured IL-2 in the media by enzyme-linked immunosorbent assay 48 h after the activation of Jurkat E6-1 cells, which were derived from a human lymphocytic cell line. These cells were activated with CD3/CD28-coated beads, which mimic the role of antigen-presenting cells during in vivo T-cell activation (Fig. 3A). Addition of erlotinib to the media resulted in a dose-dependent increase in IL-2 secretion, whereas gefitinib had little or no effect. Unfortunately, we could not determine the EC_{50} values, because the viability of the cells tended to decrease over the 48-h period in which higher concentrations of erlotinib or gefitinib were added to the media. However, these results suggest that erlotinib up-regulates secretion of IL-2 from lymphocytes at clinical concentrations.

Next, we examined the effects of erlotinib and gefitinib on lymphocytic cell migration using a Transwell chemotaxis assay system (Fig. 3B). The addition of both erlotinib and gefitinib to the media led to an increase in the number of cells attracted by chemokines; however, erlotinib activated cell migration more potently than gefitinib. In this assay, cells were incubated for 2 h, and EC_{50} values were determined.

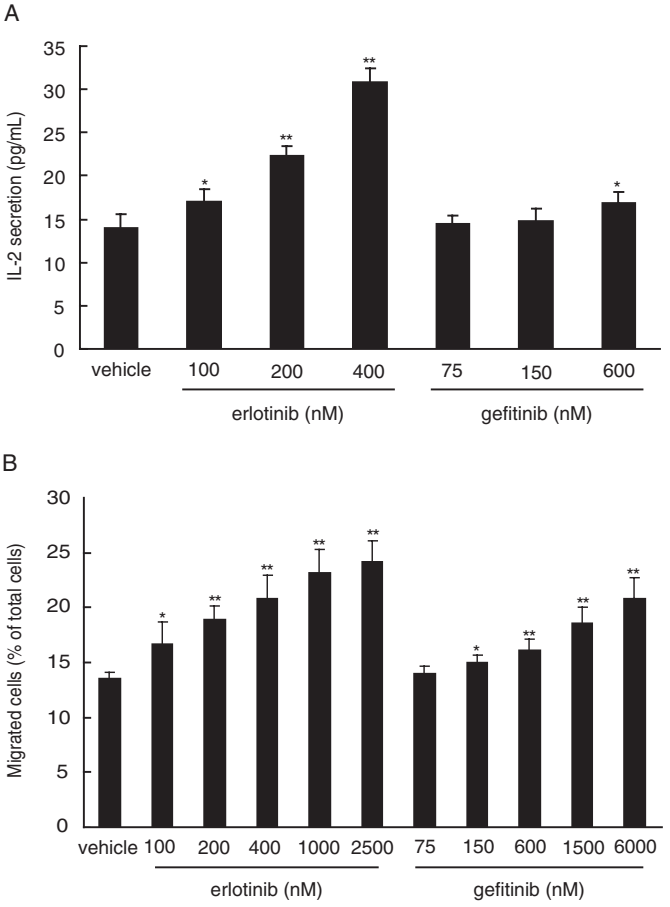

Fig. 3. Erlotinib up-regulates IL-2 secretion and cell migration in lymphocytic cells. A, effects of erlotinib and gefitinib on IL-2 secretion in Jurkat E6-1 cells stimulated with Dynabeads Human T-Activator CD3/CD28. Each data point represents the mean ± S.D. ($n = 4$). B, effects of erlotinib and gefitinib on cell migration in Jurkat E6-1 cells induced by SDF-1. Each data point represents the mean ± S.D. ($n = 4$). EC_{50} values for cell migration were 470 nM for erlotinib and 1400 nM for gefitinib. *, $P < 0.05$; **, $P < 0.01$.

The EC_{50} values for lymphocytic cell migration were 470 nM for erlotinib and 1400 nM for gefitinib. The relative E_{max} values were 1.9 for erlotinib and 1.7 for gefitinib.

STK10 Inhibition Plays a Major Role in the Up-Regulation of Lymphocytic Activation by Erlotinib. We next examined the effects of RNAi gene suppression of STK10 and SLK to further establish whether the inhibition of STK10 or SLK by erlotinib mediates the up-regulation of lymphocyte action. Knockdown efficiency was confirmed by measuring mRNA and protein levels using quantitative real-time PCR and Western blotting, respectively, in Jurkat E6-1 cells after siRNA was introduced by electroporation (Fig. 4, A and B). Because it was reported previously that IL-2 production is negatively regulated by STK10 at the transcriptional level (Tao et al., 2002), we examined the effects of gene suppression on IL-2 mRNA expression. IL-2 mRNA expression was increased 2-fold after stimulation with CD3/CD28-coated beads in Jurkat E6-1 cells treated with siSTK10 relative to cells treated with siNeg, but no significant difference was observed in cells treated with siSLK versus siNeg (Fig. 4C). Moreover, the addition of erlotinib at clinical concentrations resulted in increased IL-2 mRNA expression under SLK knockdown and control conditions; however, it did not significantly affect IL-2 mRNA under STK10 knockdown conditions (Fig. 4C). Changes in IL-2 protein in the media were consistent with these changes in mRNA (Fig. 4D). These results suggest that up-regulation of IL-2 secretion in response to erlotinib is due to transcriptional up-regulation mediated by the inhibition of STK10 by erlotinib.

We next performed a transwell migration assay using Jurkat E6-1 cells under the various siRNA conditions (Fig. 4E). STK10 knockdown increased the number of cells attracted by chemokines compared with control and SLK knockdown conditions. As was the case for IL-2 production, the addition of erlotinib to the media at clinical concentrations resulted in increased chemokine-induced cell migration, whereas no significant change was observed under STK10 knockdown conditions (Fig. 4E). These results suggest that the up-regulation of lymphocytic action by erlotinib is largely mediated by STK10 inhibition.

Erlotinib Does Not Affect the Mitogen-Activated Protein Kinase Extracellular Signal-Regulated Kinase Kinase-1 Pathway or Ca^{2+} Signaling Pathway. It has been reported that mitogen-activated protein kinase extracellular signal-regulated kinase (ERK) kinase-1 (MEK1) increases the IL-2 gene transcription (Whitehurst and Geppert, 1996). To confirm whether the modulation of MEK1 is the cause of a high level of IL-2 secretion in response to erlotinib, the involvement of MEK1 in increased IL-2 secretion by erlotinib was investigated using the MEK1-selective inhibitor PD98059. In the case of Jurkat E6-1 cells stimulated with CD3/CD28 beads, PD98059 partially inhibited the secretion of IL-2. The resistant remainder is believed to be dependent on signaling pathways other than the MEK1/ERK pathway. Moreover, erlotinib stimulated IL-2 secretion significantly even in cells cotreated with PD98059 (Fig. 5A). These results suggest that the increased IL-2 secretion induced by erlotinib treatment is mediated by the signals other than MEK1 signals. In addition, we measured the IL-2 secretion in cells under PMA/ionomycin costimulation, which bypassed the T-cell receptor (TCR) signaling to activate Ras and calcineurin (Chatila et al., 1989; Franklin et al., 1994). Upon PMA/

ionomycin cotreatment, PD98059 strongly inhibited IL-2 secretion, whereas erlotinib did not (Fig. 5B). This result suggests that IL-2 secretion triggered by PMA/ionomycin costimulation depends more strongly on MEK1 signaling than on CD3/CD28 stimulation and also suggests that erlotinib does not affect the MEK1 pathway or Ca^{2+} signaling pathway.

Administration of Erlotinib Exacerbates Irritant-Induced Skin Inflammation. Our in vitro experiments indicated that the preferential inhibition of STK10 by erlotinib enhances the lymphocytic response, leading to the aggravation of skin disorders. To confirm this, we performed an in vivo irritant hypersensitivity assay using male ddY mice. In these experiments, the swelling of earflaps 24 h after topical application of croton oil was used as an indicator of irritant hypersensitivity, and erlotinib or gefitinib was orally administered four times over 24 h. The dosage regimens for erlotinib and gefitinib were designed to maintain the inhibition rate for STK10 at a level similar to that of patients treated with these agents, based on previous reports of the mouse pharmacokinetic profiles (Marchetti et al., 2008; Wang et al., 2008) and the IC_{50} values for human and mouse STK10 measured in the present study (Fig. 2). To confirm the STK10 inhibition profiles, we measured plasma concentrations of erlotinib and gefitinib at the indicated time points and compared the estimated STK10 inhibition profiles in mice and humans (Fig. 6, A and B). Earflap swelling was significantly exacerbated by erlotinib administration compared with controls, but gefitinib administration did not affect earflap swelling (Fig. 6C).

To confirm that mouse lymphocyte responses are actually affected by erlotinib as seen in human cell line Jurkat-E6-1 cells, we also determined the effect of erlotinib and gefitinib on IL-2 secretion in vitro using lymph node cells from ddY mice. Upon stimulation with CD3/CD28 beads, the addition of erlotinib to the media resulted in a dose-dependent increase in IL-2 secretion, whereas gefitinib had no effect on lymph node cells at concentration used in clinical situations (Fig. 6D). In addition, erlotinib and gefitinib had no effect on the secretion of IL-2 in lymph node cells upon PMA/ionomycin costimulation (Fig. 6E). These results indicate that erlotinib exhibits similar lymphocytic activation properties in both Jurkat E6-1 cells and mouse lymph node cells. However, IL-2 secretion in response to PMA/ionomycin costimulation or CD3/CD28 bead stimulation was higher in lymph node cells than in Jurkat-E1 cells (Fig. 3). Several possibilities can be advanced to explain this point. Jurkat-E1 is an immortalized cell line that was cultured alone, whereas the lymph node cells were freshly isolated from mice as a mixture of several types of cells, including lymphocytes, macrophages, and dendritic cells. In general, physiological reactions of the immortalized cell line often proceed weakly compared with the case of primary cultured cells. Thus, we believe it is plausible that lymph node cells were more strongly activated than Jurkat cells, although Jurkat cells maintain their ability to produce IL-2 in response to stimulation. In addition, IL-2 production from T cells after stimulation might be up-regulated via cross-talk with other types of cells in the case of isolated lymph node cells.

Activation of Lymphocytic Responses Mediates the Exacerbation of Skin Inflammation by Erlotinib Treatment. We also measured lymphocyte infiltration in earflaps by tissue section staining. Only erlotinib treatment increased lymphocyte infiltration in the inflamed area (Fig. 7A). To confirm our in vitro finding of the up-regulation of IL-2 secretion and lymphocyte migration in response to erlotinib treatment, we

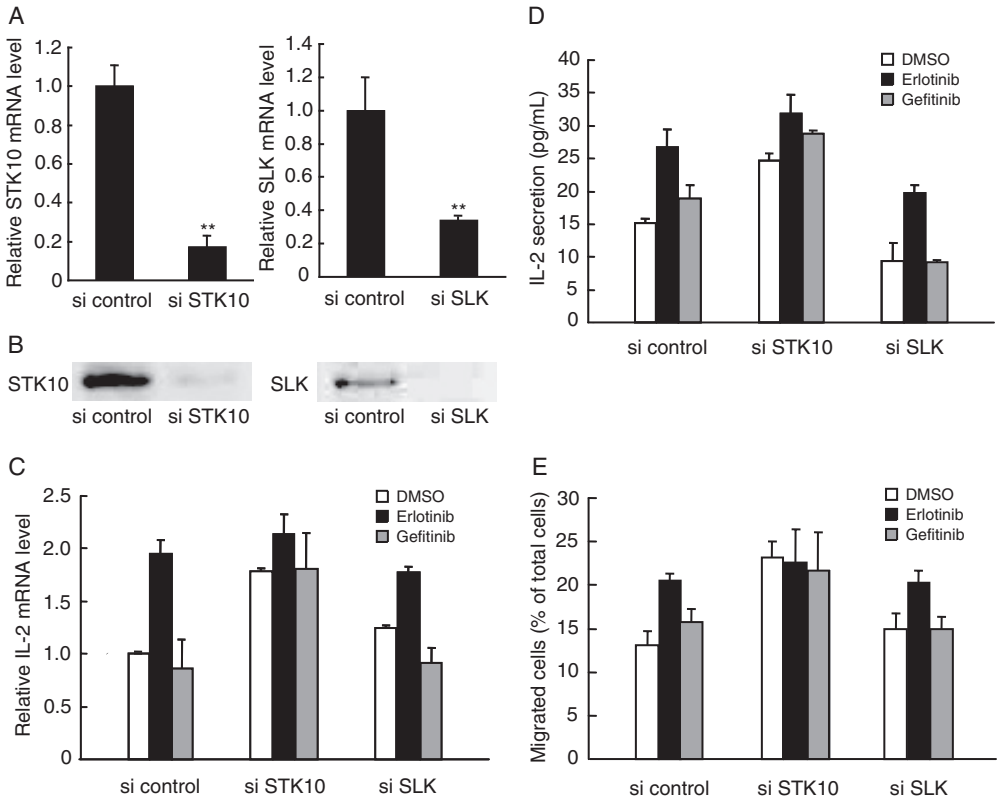

Fig. 4. STK10 inhibition plays a major role in the up-regulation of lymphocytic activity by erlotinib. A, changes of STK10 (left) and SLK (right) mRNA levels by RNAi gene suppression. Each data point represents the mean ± S.D. (n = 3). B, changes of STK10 (left) and SLK (right) protein levels by RNAi gene suppression. C, effects of RNAi gene suppression of STK10 or SLK on IL-2 mRNA expression in Jurkat E6-1 cells stimulated with beads under erlotinib or gefitinib treatment conditions. Each data point represents the mean ± S.D. (n = 3). D, effects of RNAi gene suppression of STK10 or SLK on IL-2 secretion from Jurkat E6-1 cells stimulated with beads under erlotinib or gefitinib treatment conditions. Each data point represents the mean ± S.D. (n = 3). E, effects of RNAi gene suppression of STK10 or SLK on the migration of Jurkat E6-1 cells induced by SDF-1 under erlotinib or gefitinib treatment conditions. Each data point represents the mean ± S.D. (n = 3). **, $P < 0.01$.

administered anti-IL-2 antibody or FTY720, an immunosuppressant sequestering T lymphocytes within peripheral lymphoid tissues, to mice treated with the irritant. Treatment with anti-IL-2 antibody or FTY720 reduced earflap swelling in erlotinib-treated animals (Fig. 7, B and C). These results indicate that the up-regulation of lymphocytic activation by erlotinib treatment contributes to the aggravation of skin inflammation.

Discussion

A limited number of reports have focused on the inhibition of off-target kinases by clinically used kinase inhibitors (Bain et al., 2007; Karaman et al., 2008). These reports have only addressed the magnitude of off-target K_d values or selectivity scores, which represent the ratio of off-target and primary target K_d values, and the pharmacokinetic properties of these anticancer agents have not been considered. However, the off-target kinase inhibition rate is directly correlated with the development of adverse effects. The off-target inhibition rate for a kinase inhibitor that shows 100-fold selectivity is estimated to be 8.3% if the plasma concentration of the agent is adjusted to achieve 90.0% inhibition of the primary target. It appears that 100-fold selectivity is safe enough in this case. However, if the inhibition rate for the primary target is adjusted to 99.5%, the off-target kinase inhibition rate is estimated to increase to 66.6%, possibly resulting in adverse effects. This estimation also demonstrates that the off-target inhibition rate shows large variability depending on the plasma concentration of the drug. For cytotoxic anticancer agents, clinical doses are typically determined based on the maximum tolerated dose estimation (Sleijfer and Wiemer, 2008). However, this is not always the case for tyrosine kinase inhibitors, and the primary target inhibition rates achieved at clinical doses vary among kinase inhibitors. For imatinib, the inhibition rate for Bcr-Abl, the primary target of this agent, is estimated to be 90% based on the reported IC_{50} value and the steady-state unbound plasma concentration (Deininger et al., 2005). For erlotinib and gefitinib, which are the focus of this study, the EGFR inhibition rates are estimated to be 100 and 99%, respectively (Fig. 1). Therefore, it is necessary to convert K_d or IC_{50} values for off-target kinases into inhibition rates at clinical concentrations taking into consideration the pharmacokinetic properties of tyrosine kinase inhibitors.

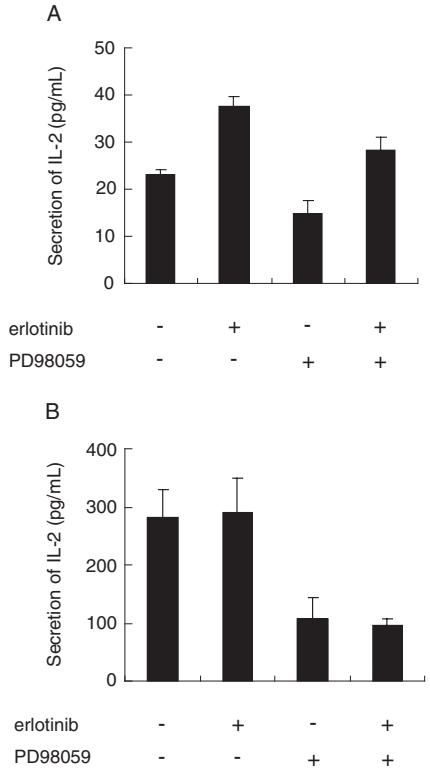

Fig. 5. Erlotinib does not affect the MEK1 pathway or Ca^{2+} signaling pathway. A, effects of the MEK1 inhibitor PD98059 on IL-2 secretion in Jurkat E6-1 cells stimulated with CD3/CD28 beads. Each data point represents the mean ± S.D. (n = 3). B, effects of the PD98059 on IL-2 secretion in Jurkat E6-1 cells stimulated with PMA/ionomycin. Each data point represents the mean ± S.D. (n = 3).

In the present study, we focused on the relationship between off-target kinase inhibition and the aggravation of skin disorders, focusing on two kinase inhibitors that primarily target EGFR, erlotinib and gefitinib. Based on estimations of human kinase occupancy by erlotinib and gefitinib, we determined that erlotinib interacts strongly with GAK, STK10, SLK, and EGFR (Fig. 1). A number of studies have described the involvement of EGFR inhibition in the pathophysiological mechanisms of cutaneous toxicity observed in patients treated with EGFR kinase inhibitors (Lacouture, 2006). The primary event is damage to the sebaceous glands and follicular epithelia, which leads to altered epidermal growth and differentiation. These cellular and structural changes subsequently trigger the release of chemokines, leading to the infiltration of mononuclear leukocytes including T lymphocytes, inflammatory dendritic cells, and macrophages to the lesion area (Guttman-Yassky et al., 2010). Histological findings show that the earliest change is the infiltration of T lymphocytes immunoreactive for CD45RO, a marker of T lymphocyte activation, which is followed by abundant neutrophil infiltration (Busam et al., 2001). T cells are believed to facilitate inflammation through a release of effector molecules (Deane and Hickey, 2009). A series of reactions, sometimes along with the bacterial infection, finally result in cutaneous injury (Guttman-Yassky et al., 2010). However, these proposed mechanisms do not fully explain the difference in the severity of skin disorders induced by erlotinib and gefitinib.

It seems unlikely that the inhibition of GAK is involved in the aggravation of skin disorder because gefitinib also interacts strongly with GAK (Fig. 1). In addition, the frequency of skin rash in patients taking lapatinib, a kinase inhibitor primarily targeting EGFR and Her2, is comparable with that in patients taking gefitinib, despite the fact that lapatinib does not interact with GAK (Karaman et al., 2008; Toi et al., 2009). In contrast, erlotinib shows a greater interaction with STK10 and SLK than with gefitinib (Fig. 1). STK10 and SLK are serine/threonine protein kinases that are closely mapped in the phylogenic tree of the Ste20 family, and STK10 is predominantly expressed in lymphocytes, whereas SLK is ubiquitously expressed (Yamada et al., 2000; Walter et al., 2003). It has been reported that STK10 negatively regulates IL-2 expression in lymphocytes at the transcriptional level and also negatively regulates cell motility through the phosphorylation of ezrin-radixin-moesin proteins (Tao et al., 2002; Belkina et al., 2009). Although there are reports that SLK is required for breast cancer cell motility, disassembly of actin stress fibers, and radial microtubule organization, little is known about the function of SLK in lymphocytes (Burakov

et al., 2008; Roovers et al., 2009). Considering these points, we selected STK10 and SLK as candidates for off-target inhibition, leading to inflammatory responses associated with the development of skin disorders using in vitro and in vivo experimental systems.

An in vitro kinase assay showed that the inhibition rates for STK10 and SLK by erlotinib in the steady state are 59 and 21%, respectively, whereas gefitinib showed only a slight inhibition of STK10 at clinical concentrations (Fig. 2). The IC_{50} values, which we determined from our in vitro experiments, were somewhat higher than the reported K_d values (Moyer et al., 1997; Albanell et al., 2002). Differences in experimental conditions might explain this difference. We determined the IC_{50} values using enzyme kinetics data obtained in the presence of 1 μM ATP, and the reported K_d values were determined using a high-throughput competitive binding assay (Karaman et al., 2008). However, we confirmed that erlotinib significantly inhibits STK10 at clinical concentrations. Our cell-based assays showed that erlotinib enhances lymphocytic responses such as IL-2 secretion and cell migration (Fig. 3). The EC_{50} values of erlotinib and gefitinib for the enhancement of cell migration were comparable with the IC_{50} values for STK10 inhibition (Fig. 3). In addition, RNAi gene suppression experiments indicated that the up-regulation of lymphocytic activity by erlotinib or gefitinib is primarily mediated by STK10 inhibition (Fig. 4). We obtained similar results by using kinase dead forms of STK10 and SLK in place of siRNA (data not shown). Considering these in vitro results, it can be hypothesized that the preferential inhibition of STK10 by erlotinib leads to enhanced lymphocyte migration to the lesion area and increased local IL-2 secretion.

T-cell activation is induced by a series of intracellular signaling cascade initiated by signals from the TCR/CD3 complex and other costimulatory molecules including CD28 (Clevers et al., 1988). CD28 provides an essential costimulatory signal that approximates T cell and antigen-presenting cells and augments the production of IL-2 (Lenschow et al., 1996). In our present study, we used CD3/CD28 beads stim-

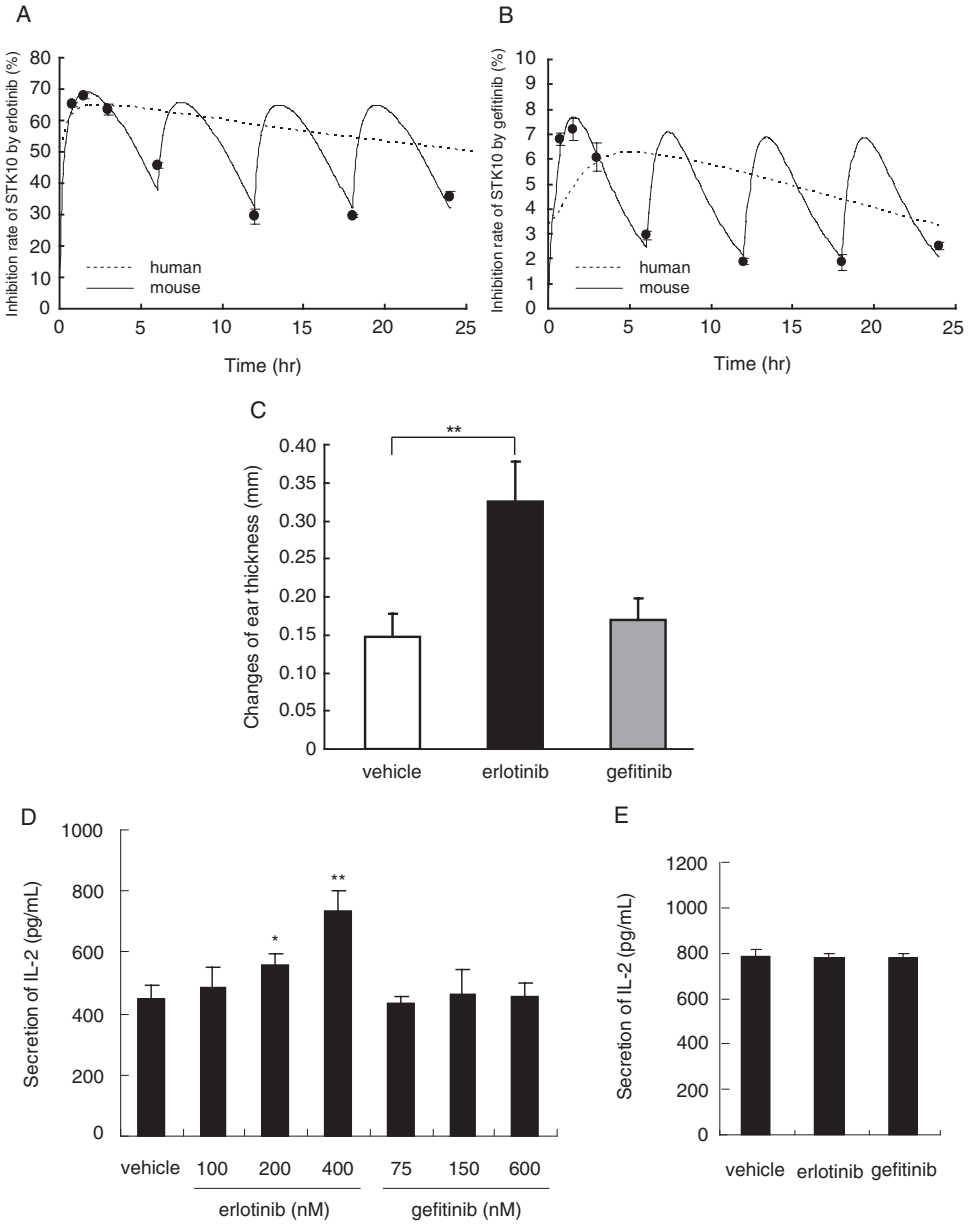

Fig. 6. Erlotinib exacerbates the skin inflammatory response to croton oil. Inhibition ratios of STK10 in ddY mice orally administered erlotinib (A) or gefitinib (B). Each data point represents the mean ± S.D. (n = 5). The solid line represents the fitted inhibition rate profile of mSTK10 by erlotinib in the mouse model, and the dashed line represents the predicted inhibition rate profile of hSTK10 by erlotinib under human clinical conditions. C, effects of erlotinib or gefitinib administration on changes in earflap swelling. Each data point represents the mean ± S.D. (n = 5). *, $P < 0.05$; **, $P < 0.01$. D, effects of erlotinib and gefitinib on IL-2 secretion in mouse lymph node cells stimulated with Dynabeads Mouse T-Activator CD3/CD28. Each data point represents the mean ± S.D. (n = 4). E, effects of erlotinib and gefitinib on IL-2 secretion in mouse lymph node cells stimulated with PMA/ionomycin. Each data point represents the mean ± S.D. (n = 4).

ulation, which mimics natural TCR signaling. TCR signaling is further amplified by 70-kDa ζ-chain-associated protein kinase, which leads to the activation of multiple pathways, including ERK, c-Jun NH_2-terminal kinase, nuclear factor-κB, p38, and nuclear factor of activated T cells, which ultimately induce IL-2 gene expression (Chu et al., 1998). Meanwhile, costimulation with PMA/ionomycin bypasses the TCR signaling and activates the signaling downstream of phospholipase Cγ, a downstream effector of 70-kDa ζ-chain-associated protein kinase (Chatila et al., 1989; Franklin et al., 1994). Because erlotinib could up-regulate the IL-2 secretion under the CD3/CD28 stimulation not upon PMA/ionomycin stimulation (Fig. 5, A and B), up-regulation of IL-2 secretion by erlotinib via STK10 inhibition could be dependent on the signals other than the downstream signals of phospholipase Cγ. These results are consistent with previous reports that STK10 down-regulates the IL-2 secretion upon Raji/SEE stimulation but not upon PMA/ionomycin cotreatment. The authors of this report considered that STK10 might act on early events in T-cell activation (Tao et al., 2002).

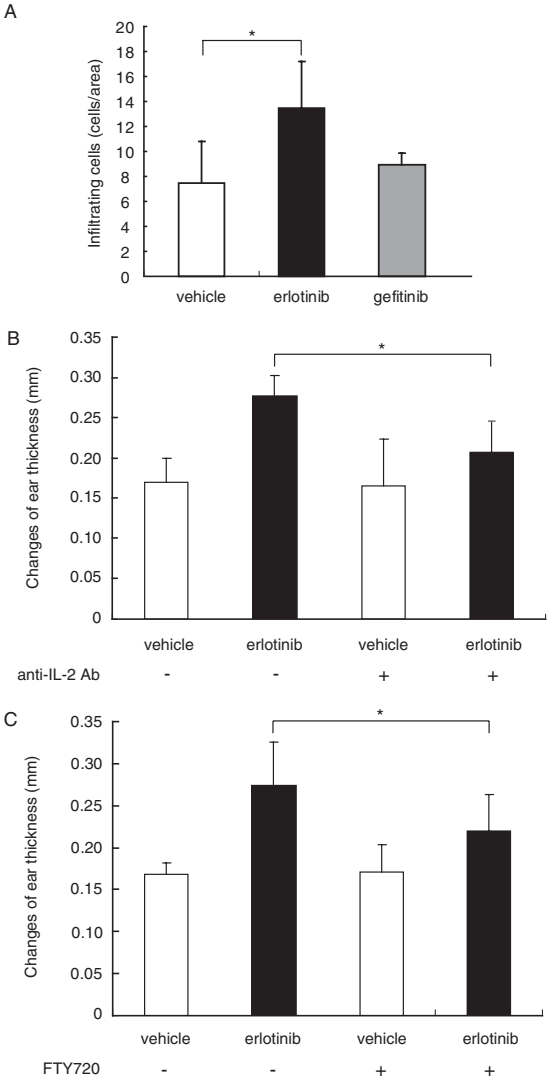

Fig. 7. IL-2 secretion and lymphocyte infiltration contribute to the aggravation of the inflammatory response by erlotinib. A, effects of erlotinib or gefitinib administration on earflap lymphocyte infiltration. Each data point represents the mean ± S.D. (n = 3). B, effects of anti-IL-2 Ab on earflap swelling aggravated by erlotinib treatment. Each data point represents the mean ± S.D. (n = 6). C, effects of FTY720 on the earflap swelling aggravated by erlotinib treatment. Each data point represents the mean ± S.D. (n = 8). *, $P < 0.05$.

Our observations in a mouse contact hypersensitivity model were consistent with the in vitro observations (Figs. 6 and 7). Infiltration of lymphocytes was up-regulated in the earflaps of erlotinib-treated mice compared with gefitinib- or control-treated animals (Fig. 7). Treatment with anti-IL-2 antibody or FTY720 also resulted in a reduction in earflap swelling induced by erlotinib treatment (Fig. 7). These observations are also consistent with the proposed mechanism of skin rash development in patients treated with erlotinib, in which inflammatory reactions are dominated by mononuclear leukocytes, including lymphocytes and neutrophils (Guttman-Yassky et al., 2010).

It has been reported that there is significant interindividual variation in plasma concentrations of erlotinib and gefitinib (Li et al., 2006; Thomas et al., 2009). Preclinical studies have demonstrated that CYP3A4 is primarily involved in the metabolism of erlotinib and gefitinib, and therefore, pharmacokinetic interactions may take place with drugs that inhibit or induce CYP3A4 (McKillop et al., 2005; Li et al., 2007). Itraconazole is a potent inhibitor of CYP3A4 and the plasma area under the curve of gefitinib was reported to increase by 78% with the coadministration of itraconazole (Swaisland et al., 2005). Coadministration of ketoconazole, another strong inhibitor of CYP3A4, was reported to cause a 2-fold increase in plasma area under the curve and the maximum plasma concentration of erlotinib (Rakhit et al., 2008). Based on the IC_{50} values obtained from our in vitro kinase assay and the mean unbound plasma concentrations of erlotinib and gefitinib at the steady state, it is estimated that the mean rate of STK10 inhibition was approximately 59% for erlotinib but only 4% for gefitinib (Fig. 2). If interindividual variations in CYP3A4 activity and/or drug-drug interactions were to result in a 2-fold higher unbound plasma concentration of erlotinib or gefitinib compared with the mean values, the inhibition rate for STK10 would increase to 74% for erlotinib but would remain at 8% for gefitinib. In contrast, the inhibition rate for EGFR, which is almost 100% for both erlotinib and gefitinib, would not be affected by these conditions. These estimations indicate that interindividual differences in the severity of skin rash among patients treated with erlotinib may be due to interindividual variability in the STK10 inhibition rate. This hypothesis is also supported by a previous report showing that variability in skin rash susceptibility was associated with trough erlotinib plasma concentrations (Rudin et al., 2008).

In conclusion, we propose a mechanism in which erlotinib exacerbates skin disorders through the enhancement of lymphocytic responses such as lymphocyte migration and increased IL-2 secretion via STK10 inhibition. Because it has been demonstrated that off-target inhibition by kinase inhibitors can result in the development of adverse effects under clinical conditions, it would be beneficial to determine the comprehensive inhibitory profiles of kinase inhibitors at the preclinical stage. In cases in which the inhibition rate for off-target kinases is predicted to be variable within the clinical concentration range for reasons such as interindividual variability in pharmacokinetics and drug-drug interactions, clinical dose determination studies should be performed carefully and strategically to maximize therapeutic effects and minimize side effects.

Authorship Contributions

Participated in research design: Yamamoto, Honma, and Suzuki.
Conducted experiments: Yamamoto and Honma.
Performed data analysis: Yamamoto and Honma.
Wrote or contributed to the writing of the manuscript: Yamamoto, Honma, and Suzuki.

References

Albanell J, Rojo F, Averbuch S, Feyereislova A, Mascaro JM, Herbst R, LoRusso P, Rischin D, Sauleda S, Gee J, et al. (2002) Pharmacodynamic studies of the epidermal growth factor receptor inhibitor ZD1839 in skin from cancer patients: histopathologic and molecular consequences of receptor inhibition. *J Clin Oncol* **20:**110–124.

Bain J, Plater L, Elliott M, Shpiro N, Hastie CJ, McLauchlan H, Klevernic I, Arthur JS, Alessi DR, and Cohen P (2007) The selectivity of protein kinase inhibitors: a further update. *Biochem J* **408:**297–315.

Belkina NV, Liu Y, Hao JJ, Karasuyama H, and Shaw S (2009) LOK is a major ERM kinase in resting lymphocytes and regulates cytoskeletal rearrangement through ERM phosphorylation. *Proc Natl Acad Sci USA* **106:**4707–4712.

Bonner JA, Harari PM, Giralt J, Azarnia N, Shin DM, Cohen RB, Jones CU, Sur R, Raben D, Jassem J, et al. (2006) Radiotherapy plus cetuximab for squamous-cell carcinoma of the head and neck. *N Engl J Med* **354:**567–578.

Burakov AV, Zhapparova ON, Kovalenko OV, Zinovkina LA, Potekhina ES, Shanina NA, Weiss DG, Kuznetsov SA, and Nadezhdina ES (2008) Ste20-related protein kinase LOSK (SLK) controls microtubule radial array in interphase. *Mol Biol Cell* **19:**1952–1961.

Busam KJ, Capodieci P, Motzer R, Kiehn T, Phelan D, and Halpern AC (2001) Cutaneous side-effects in cancer patients treated with the antiepidermal growth factor receptor antibody C225. *Br J Dermatol* **144:**1169–1176.

Chatila T, Silverman L, Miller R, and Geha R (1989) Mechanisms of T cell activation by the calcium ionophore ionomycin. *J Immunol* **143:**1283–1289.

Chu DH, Morita CT, and Weiss A (1998) The Syk family of protein tyrosine kinases in T-cell activation and development. *Immunol Rev* **165:**167–180.

Clevers H, Alarcon B, Wileman T, and Terhorst C (1988) The T cell receptor/CD3 complex: a dynamic protein ensemble. *Annu Rev Immunol* **6:**629–662.

Deane JA and Hickey MJ (2009) Molecular mechanisms of leukocyte trafficking in T-cell-mediated skin inflammation: insights from intravital imaging. *Expert Rev Mol Med* **11:**e25.

Deininger M, Buchdunger E, and Druker BJ (2005) The development of imatinib as a therapeutic agent for chronic myeloid leukemia. *Blood* **105:**2640–2653.

Franklin RA, Tordai A, Patel H, Gardner AM, Johnson GL, and Gelfand EW (1994) Ligation of the T cell receptor complex results in activation of the Ras/Raf-1/MEK/MAPK cascade in human T lymphocytes. *J Clin Invest* **93:**2134–2140.

Fukuoka M, Yano S, Giaccone G, Tamura T, Nakagawa K, Douillard JY, Nishiwaki Y, Vansteenkiste J, Kudoh S, Rischin D, et al. (2003) Multi-institutional randomized phase II trial of gefitinib for previously treated patients with advanced non-small-cell lung cancer (The IDEAL 1 Trial) [published erratum appears in *J Clin Oncol* **22:**4811, 2004]. *J Clin Oncol* **21:**2237–2246.

Geyer CE, Forster J, Lindquist D, Chan S, Romieu CG, Pienkowski T, Jagiello-Gruszfeld A, Crown J, Chan A, Kaufman B, et al. (2006) Lapatinib plus capecitabine for HER2-positive advanced breast cancer. *N Engl J Med* **355:**2733–2743.

Guttman-Yassky E, Mita A, De Jonge M, Matthews L, McCarthy S, Iwata KK, Verweij J, Rowinsky EK, and Krueger JG (2010) Characterisation of the cutaneous pathology in non-small cell lung cancer (NSCLC) patients treated with the EGFR tyrosine kinase inhibitor erlotinib. *Eur J Cancer* **46:**2010–2019.

Hidalgo M, Siu LL, Nemunaitis J, Rizzo J, Hammond LA, Takimoto C, Eckhardt SG, Tolcher A, Britten CD, Denis L, et al. (2001) Phase I and pharmacologic study of OSI-774, an epidermal growth factor receptor tyrosine kinase inhibitor, in patients with advanced solid malignancies. *J Clin Oncol* **19:**3267–3279.

Karaman MW, Herrgard S, Treiber DK, Gallant P, Atteridge CE, Campbell BT, Chan KW, Ciceri P, Davis MI, Edeen PT, et al. (2008) A quantitative analysis of kinase inhibitor selectivity. *Nat Biotechnol* **26:**127–132.

Kari C, Chan TO, Rocha de Quadros M, and Rodeck U (2003) Targeting the epidermal growth factor receptor in cancer: apoptosis takes center stage. *Cancer Res* **63:**1–5.

Kerkela R, Woulfe KC, Durand JB, Vagnozzi R, Kramer D, Chu TF, Beahm C, Chen MH, and Force T (2009) Sunitinib-induced cardiotoxicity is mediated by off-target inhibition of AMP-activated protein kinase. *Clin Transl Sci* **2:**15–25.

Kris MG, Natale RB, Herbst RS, Lynch TJ Jr, Prager D, Belani CP, Schiller JH, Kelly K, Spiridonidis H, Sandler A, et al. (2003) Efficacy of gefitinib, an inhibitor of the epidermal growth factor receptor tyrosine kinase, in symptomatic patients with non-small cell lung cancer: a randomized trial. *JAMA* **290:**2149–2158.

Lacouture ME (2006) Mechanisms of cutaneous toxicities to EGFR inhibitors. *Nat Rev Cancer* **6:**803–812.

Lenschow DJ, Walunas TL, and Bluestone JA (1996) CD28/B7 system of T cell costimulation. *Annu Rev Immunol* **14:**233–258.

Li J, Karlsson MO, Brahmer J, Spitz A, Zhao M, Hidalgo M, and Baker SD (2006) CYP3A phenotyping approach to predict systemic exposure to EGFR tyrosine kinase inhibitors. *J Natl Cancer Inst* **98:**1714–1723.

Li J, Zhao M, He P, Hidalgo M, and Baker SD (2007) Differential metabolism of gefitinib and erlotinib by human cytochrome P450 enzymes. *Clin Cancer Res* **13:**3731–3737.

Marchetti S, de Vries NA, Buckle T, Bolijn MJ, van Eijndhoven MA, Beijnen JH, Mazzanti R, van Tellingen O, and Schellens JH (2008) Effect of the ATP-binding cassette drug transporters ABCB1, ABCG2, and ABCC2 on erlotinib hydrochloride (Tarceva) disposition in in vitro and in vivo pharmacokinetic studies employing Bcrp1−/−/Mdr1a/1b−/− (triple-knockout) and wild-type mice. *Mol Cancer Ther* **7:**2280–2287.

Mascia F, Mariani V, Girolomoni G, and Pastore S (2003) Blockade of the EGF receptor induces a deranged chemokine expression in keratinocytes leading to enhanced skin inflammation. *Am J Pathol* **163:**303–312.

McKillop D, McCormick AD, Millar A, Miles GS, Phillips PJ, and Hutchison M (2005) Cytochrome P450-dependent metabolism of gefitinib. *Xenobiotica* **35:**39–50.

Moyer JD, Barbacci EG, Iwata KK, Arnold L, Boman B, Cunningham A, DiOrio C, Doty J, Morin MJ, Moyer MP, et al. (1997) Induction of apoptosis and cell cycle arrest by CP-358,774, an inhibitor of epidermal growth factor receptor tyrosine kinase. *Cancer Res* **57:**4838–4848.

Nakagawa K, Tamura T, Negoro S, Kudoh S, Yamamoto N, Yamamoto N, Takeda K, Swaisland H, Nakatani I, Hirose M, et al. (2003) Phase I pharmacokinetic trial of the selective oral epidermal growth factor receptor tyrosine kinase inhibitor gefitinib ('Iressa', ZD1839) in Japanese patients with solid malignant tumors. *Ann Oncol* **14:**922–930.

Pallis AG, Mavroudis D, Androulakis N, Souglakos J, Kouroussis C, Bozionelou V, Vlachonikolis IG, and Georgoulias V (2003) ZD1839, a novel, oral epidermal growth factor receptor-tyrosine kinase inhibitor, as salvage treatment in patients with advanced non-small cell lung cancer. Experience from a single center participating in a compassionate use program. *Lung Cancer* **40:**301–307.

Rakhit A, Pantze MP, Fettner S, Jones HM, Charoin JE, Riek M, Lum BL, and Hamilton M (2008) The effects of CYP3A4 inhibition on erlotinib pharmacokinetics: computer-based simulation (SimCYP) predicts in vivo metabolic inhibition. *Eur J Clin Pharmacol* **64:**31–41.

Roovers K, Wagner S, Storbeck CJ, O'Reilly P, Lo V, Northey JJ, Chmielecki J, Muller WJ, Siegel PM, and Sabourin LA (2009) The Ste20-like kinase SLK is required for ErbB2-driven breast cancer cell motility. *Oncogene* **28:**2839–2848.

Rudin CM, Liu W, Desai A, Karrison T, Jiang X, Janisch L, Das S, Ramirez J, Poonkuzhali B, Schuetz E, et al. (2008) Pharmacogenomic and pharmacokinetic determinants of erlotinib toxicity. *J Clin Oncol* **26:**1119–1127.

Rusnak DW, Lackey K, Affleck K, Wood ER, Alligood KJ, Rhodes N, Keith BR, Murray DM, Knight WB, Mullin RJ, et al. (2001) The effects of the novel, reversible epidermal growth factor receptor/ErbB-2 tyrosine kinase inhibitor, GW2016, on the growth of human normal and tumor-derived cell lines in vitro and in vivo. *Mol Cancer Ther* **1:**85–94.

Segaert S and Van Cutsem E (2005) Clinical signs, pathophysiology and management of skin toxicity during therapy with epidermal growth factor receptor inhibitors. *Ann Oncol* **16:**1425–1433.

Shepherd FA, Rodrigues Pereira J, Ciuleanu T, Tan EH, Hirsh V, Thongprasert S, Campos D, Maoleekoonpiroj S, Smylie M, Martins R, et al. (2005) Erlotinib in previously treated non-small-cell lung cancer. *N Engl J Med* **353:**123–132.

Sleijfer S and Wiemer E (2008) Dose selection in phase I studies: why we should always go for the top. *J Clin Oncol* **26:**1576–1578.

Swaisland HC, Ranson M, Smith RP, Leadbetter J, Laight A, McKillop D, and Wild MJ (2005) Pharmacokinetic drug interactions of gefitinib with rifampicin, itraconazole and metoprolol. *Clin Pharmacokinet* **44:**1067–1081.

Tao L, Wadsworth S, Mercer J, Mueller C, Lynn K, Siekierka J, and August A (2002) Opposing roles of serine/threonine kinases MEKK1 and LOK in regulating the CD28 responsive element in T-cells. *Biochem J* **363:**175–182.

Thomas F, Rochaix P, White-Koning M, Hennebelle I, Sarini J, Benlyazid A, Malard L, Lefebvre JL, Chatelut E, and Delord JP (2009) Population pharmacokinetics of erlotinib and its pharmacokinetic/pharmacodynamic relationships in head and neck squamous cell carcinoma. *Eur J Cancer* **45:**2316–2323.

Toi M, Iwata H, Fujiwara Y, Ito Y, Nakamura S, Tokuda Y, Taguchi T, Rai Y, Aogi K, Arai T, et al. (2009) Lapatinib monotherapy in patients with relapsed, advanced, or metastatic breast cancer: efficacy, safety, and biomarker results from Japanese patients phase II studies. *Br J Cancer* **101:**1676–1682.

Van Cutsem E, Peeters M, Siena S, Humblet Y, Hendlisz A, Neyns B, Canon JL, Van Laethem JL, Maurel J, Richardson G, et al. (2007) Open-label phase III trial of panitumumab plus best supportive care compared with best supportive care alone in patients with chemotherapy-refractory metastatic colorectal cancer. *J Clin Oncol* **25:**1658–1664.

Vandyke K, Fitter S, Dewar AL, Hughes TP, and Zannettino AC (2010) Dysregulation of bone remodeling by imatinib mesylate. *Blood* **115:**766–774.

Walter SA, Cutler RE Jr, Martinez R, Gishizky M, and Hill RJ (2003) Stk10, a new member of the polo-like kinase kinase family highly expressed in hematopoietic tissue. *J Biol Chem* **278:**18221–18228.

Wang S, Guo P, Wang X, Zhou Q, and Gallo JM (2008) Preclinical pharmacokinetic/pharmacodynamic models of gefitinib and the design of equivalent dosing regimens in EGFR wild-type and mutant tumor models. *Mol Cancer Ther* **7:**407–417.

Whitehurst CE and Geppert TD (1996) MEK1 and the extracellular signal-regulated kinases are required for the stimulation of IL-2 gene transcription in T cells. *J Immunol* **156:**1020–1029.

Woodworth CD, Michael E, Marker D, Allen S, Smith L, and Nees M (2005) Inhibition of the epidermal growth factor receptor increases expression of genes that stimulate inflammation, apoptosis, and cell attachment. *Mol Cancer Ther* **4:**650–658.

Yamada E, Tsujikawa K, Itoh S, Kameda Y, Kohama Y, and Yamamoto H (2000) Molecular cloning and characterization of a novel human STE20-like kinase, hSLK. *Biochim Biophys Acta* **1495:**250–262.

Yamamoto N, Horiike A, Fujisaka Y, Murakami H, Shimoyama T, Yamada Y, and Tamura T (2008) Phase I dose-finding and pharmacokinetic study of the oral epidermal growth factor receptor tyrosine kinase inhibitor Ro50–8231 (erlotinib) in Japanese patients with solid tumors. *Cancer Chemother Pharmacol* **61:**489–496.

Address correspondence to: Dr. Masashi Honma, Department of Pharmacy, The University of Tokyo Hospital, Faculty of Medicine, The University of Tokyo, 7-3-1 Hongo, Bunkyo-ku, Tokyo 113-8655, Japan. E-mail: mhonmatky@umin.ac.jp.